The rapid solidification of Ti_3Al : a molecular dynamics study

2004 J. Phys.: Condens. Matter 16 4203

(http://iopscience.iop.org/0953-8984/16/24/002)

INSTITUTE OF PHYSICS PUBLISHING JOURNAL OF PHYSICS: CONDENSED MATTER

J. Phys.: Condens. Matter **16** (2004) 4203–4210 PII: S0953-8984(04)76359-6

The rapid solidification of Ti_3Al: a molecular dynamics study

Q X Pei[1,3], C Lu[1] and M W Fu[2]

[1] Institute of High Performance Computing, 1 Science Park Road, Singapore 117528, Singapore
[2] Singapore Institute of Manufacturing Technology, 71 Nanyang Drive, Singapore 638075, Singapore

E-mail: peiqx@ihpc.a-star.edu.sg

Received 16 February 2004
Published 4 June 2004
Online at stacks.iop.org/JPhysCM/16/4203
doi:10.1088/0953-8984/16/24/002

Abstract

The rapid solidification of Ti_3Al was studied with the constant-pressure and constant-temperature molecular dynamics (NPT-MD) technique to obtain an atomistic description of glass formation and crystallization in the alloy. The embedded atom method (EAM) potential for the Ti–Al binary system recently developed by Zope and Mishin (2003 *Phys. Rev.* B **68** 024102) was applied in the simulations. The effects of different cooling rates on the glass formation and crystallization of liquid Ti_3Al were studied. In addition, the crystallization of the amorphous Ti_3Al as a function of increasing temperature was also studied. The calculated internal energy change and radial distribution function during cooling and heating processes provided a good picture of the structural transformations, and the results were consistent with the results obtained experimentally.

(Some figures in this article are in colour only in the electronic version)

1. Introduction

Rapid solidification usually refers to the solidification at a much higher cooling rate than the conventional cooling rates of less than about 10^2 K s^{-1} [1]. The rapid solidification technique has been used to produce materials with improved mechanical and physical properties [1, 2]. It is well known that when liquid metal is cooled down, either crystalline solid or amorphous solid will be formed depending on the cooling rate. If the cooling rate is high enough, there is little time for the crystalline phase to nucleate and grow, and thus the metastable amorphous structure (metallic glass) will be obtained.

[3] Author to whom any correspondence should be addressed.

Molecular dynamics (MD) simulation is widely used in materials research, and it has also been used by some researchers in studying the structural development of some pure metals and binary alloys during rapid solidification processes [3–10]. MD can describe the structural change in the glass transition and crystallization processes. The cooling rate used in MD simulations can be similar or beyond what is achievable in laboratory rapid quenching experiments. The MD results can thus provide insight into the local structural features and the corresponding thermal dynamics properties possibly present in the experimental metals under various quenching conditions.

However, the reliability of MD simulation results greatly depends on the quality of the interatomic potential employed. For a metallic system, a many-body potential, instead of a pair potential, has to be used to consider the many-body effect due to metallic bonding. Therefore, a semiempirical many-body potential based on the embedded atom method (EAM) [11], or the equivalent Finnis–Sinclair approach [12], has been used in MD simulations for pure metals and alloys. Since EAM was first proposed by Daw and Baskes [13, 14] about twenty years ago, the EAM potentials for many pure metals and a limited number of binary alloys have been constructed by fitting to experimental data. However, recent studies [15, 16] have shown that the incorporation of *ab initio* data into the construction of interatomic potentials can significantly enhance their ability to mimic the interatomic interactions.

Very recently, Zope and Mishin [17] developed the EAM potential for the Ti–Al system by fitting to a large database of both experimental and *ab initio* data. Ti–Al alloys are interesting because they have great potential for high-temperature applications in aerospace and automobile industries due to their excellent mechanical and physical properties such as high strength, low density, good oxidation and corrosion resistance.

With this newly developed EAM potential for the Ti–Al system, we carried out molecular dynamics simulations to study the structural change of Ti_3Al during rapid cooling and heating processes. Both the glass formation and crystallization during cooling processes and the crystallization and melting during heating processes were investigated.

2. Simulation conditions

A constant-pressure and constant-temperature molecular dynamics (NPT-MD) technique was used with the external pressure being kept at 1 atm. The simulations were performed on a system of 8000 atoms (6000 Ti atoms and 2000 Al atoms, which corresponds to the composition of Ti_3Al) in a cubic cell under periodic boundary conditions. The equations of motion were solved using a fourth-order gear predictor–corrector algorithm with a time step $\Delta t = 5.0$ fs ($1\ \text{fs} = 10^{-15}$ s).

The simulations were started at 2000 K, which was about 100 K higher than the melting point of the intermetallic compound Ti_3Al. The system was run for 100 000 time steps at this starting temperature to guarantee an equilibrium liquid state. Then the system was cooled down to below room temperature at different quenching rates ranging from 1.0 to 100 K ps^{-1} ($1\ \text{ps} = 10^{-12}$ s). Due to the difference in cooling rates, amorphous or crystalline solids might be formed. Then the obtained amorphous and crystalline solids were heated up again to 2000 K with a heating rate of 1.0 K ps^{-1}. The cooling or heating processes were realized by executing stepwise temperature changes with a temperature step of 50 K. The system temperature was kept at the desired value by scaling the atoms' velocities. The initial velocities of the atoms were determined according to the initial temperature of 2000 K and assuming that they follow the Maxwell–Boltzmann distribution.

The simulation results were analysed by the atom trajectory, internal energy change, and radial distribution function (RDF). RDF, or $g(r)$ in some papers, is a very important structural

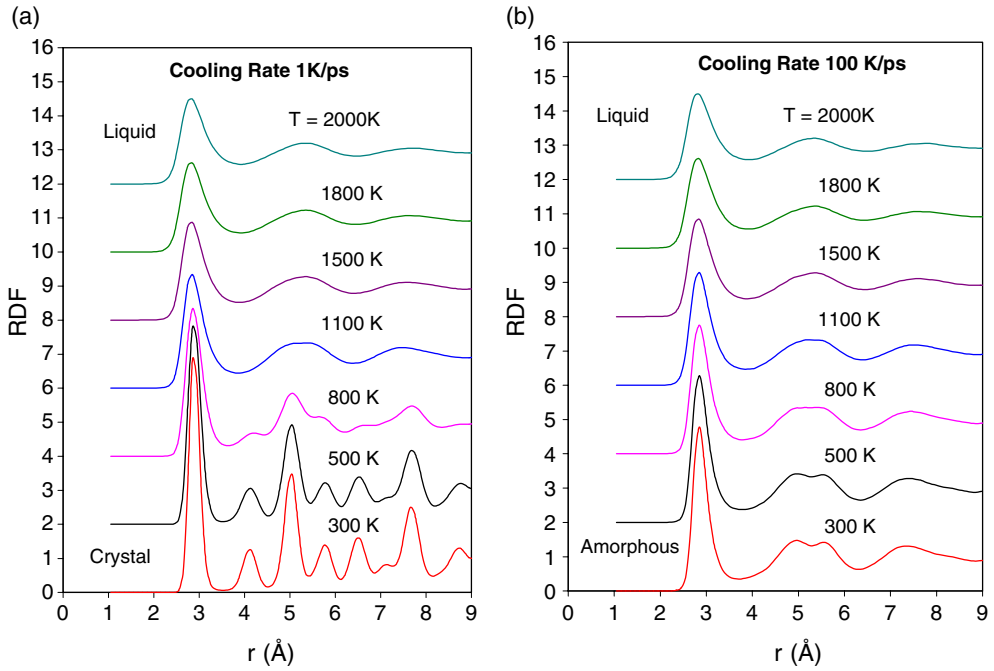

Figure 1. The temperature dependence of the radial distribution function (RDF) of Ti_3Al when cooled down at the rate of 1 K ps^{-1} (a) and 100 K ps^{-1} (b). The values of the RDF coordinates are correct for the 300 K curve; the curves for the higher temperatures are shifted up by 2–12 units.

parameter, which shows the structural characteristics of the atoms' system, such as the ordering degree of the atoms. It is defined as the probability of finding a pair of molecules a distance r apart, relative to the probability expected for a completely random distribution at the same density. Thus, RDF is a normalized parameter and its value should go to 1 with large r for liquid metal.

3. Simulation results and discussion

Figure 1 shows the RDF of Ti_3Al during the cooling processes at the two rapid cooling rates of 1 and 100 K ps^{-1}, respectively. It can be seen that at 2000 K the RDF shows the general shape of the liquid state, which was observed in experiments [18]. As the temperature drops, the first peak in the RDF grows higher and the valley becomes deeper, which shows that the disordering degree in the liquid metal decreases and the ordering degree increases. When cooling down at the slow quenching rate of 1 K ps^{-1}, see figure 1(a), the first peak becomes very high and many small peaks appear, which shows that crystallization has happened and the final phase is a crystalline structure. When cooling down at the fast quenching rate of 100 K ps^{-1}, see figure 1(b), the second peak splits into two subpeaks, which indicates the formation of metallic glass. The split of the second peak is a well-known feature of amorphous structure [18].

The final atomic configurations at room temperature (300 K) after cooling down at the above two cooling rates are shown in figure 2. The obtained crystalline structure and amorphous structure can be further confirmed from the figures. It can be seen in figure 2(a) that the atoms are closely and orderly distributed for the cooling rate of 1 K ps^{-1}, which shows a crystalline structure. However, it can be seen in figure 2(b) that the atoms are loosely and disorderly

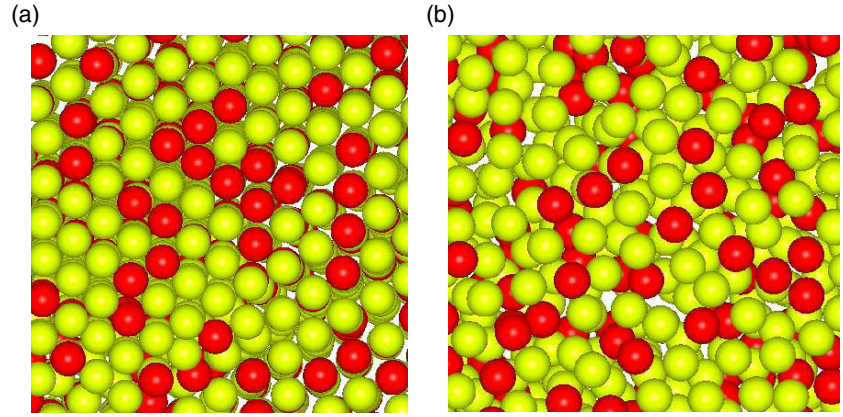

Figure 2. The crystalline structure (a) and the amorphous structure (b) at room temperature obtained at the quenching rates of 1 and 100 K ps^{-1} respectively. The dark balls are Al atoms.

distributed for the cooling rate of 100 K ps^{-1}, which shows an amorphous structure. It should be pointed out that the crystalline structure obtained with the cooling rate of 1 K ps^{-1} is not a perfectly ordered $D0_{19}$ lattice, which is a typical structure for the Ti_3Al compound. This is because the cooling rate is so high that the atoms do not have enough time to rearrange themselves into the perfect $D0_{19}$ crystal structure.

The atomic volumes of the crystalline and amorphous structures shown in figure 2 are 17.37 and 17.88 Å^3 respectively. Here, the atomic volume is calculated as the cell volume divided by the number of atoms in the cell. These values show that the volume of the crystalline structure is smaller than the volume of the amorphous structure, which is due to the orderly distribution of the atoms in the crystalline structure. However, the atomic volume of the simulated crystalline structure is higher than the experimental value of 16.81 Å^3 [19]. This difference may result from the rapid solidification process. With slower cooling rate, the simulated crystalline volume will be closer to the experimental value characterizing the equilibrium phase.

The internal energy change as a function of temperature for all the rapid cooling rates investigated is shown in figure 3. In the high temperature region, the internal energy drops linearly with decreasing temperature and there is little difference in the internal energy changes between the different cooling rates. This shows that at high temperature, the atoms are mobile enough to follow the temperature drop regardless of the temperature falling speeds investigated. In the low temperature region when the temperature is below about 1000 K, the internal energy change shows a big difference between the different cooling rates. For the slow quenching rates of 1.0 and 1.5 K ps^{-1}, there is a sharp drop of internal energy, which indicates that liquid-to-crystallization transition has happened. The crystallization temperature can be defined from the energy curves in figure 3, which shows that T_{c1} is about 1000 K and T_{c2} is about 950 K. However, for the fast quenching rates of 3.0 K ps^{-1} and above, there is no sharp drop of internal energy, only the slope of internal energy curves becomes lower in the low temperature region. The discontinuity in slope indicates a liquid-to-amorphous transition or a glass transition. Thus, the glass transition temperature T_g for the different cooling rates are obtained from the internal energy curves as shown in figure 3.

The glass transition temperature can also be defined by the Wendt–Abraham parameter $R = g_{min}/g_{max}$ [20], where g_{min} and g_{max} are the magnitudes of the first minimum and maximum in the RDF, respectively. The calculated R versus temperature is shown in figure 4.

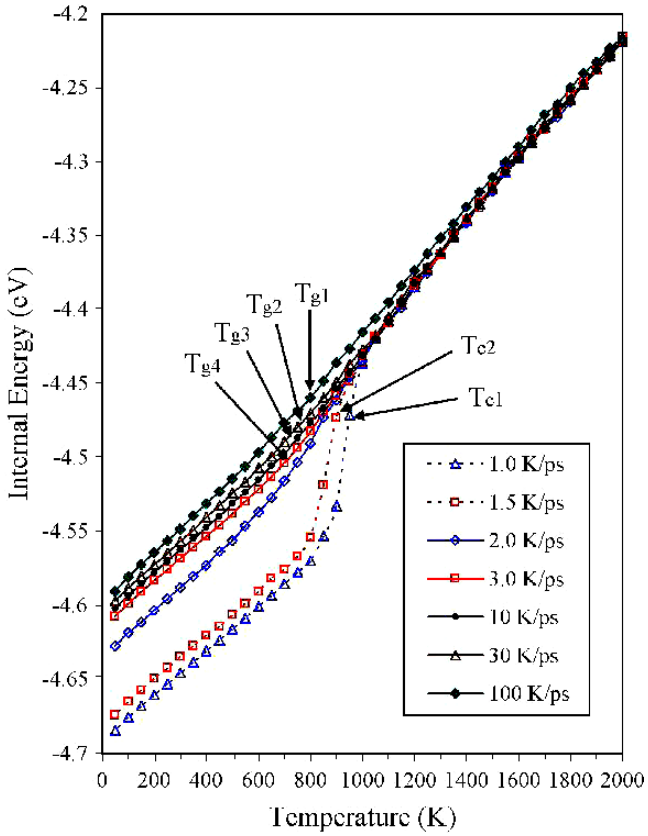

Figure 3. Variation of internal energy during cooling for different quenching rates. The glass transition temperatures (T_g) and the crystallization temperatures (T_c) are indicated by arrows.

The slope change in the R curves shows the glass transition temperatures during quenching. Both figures 3 and 4 show that the glass transition temperatures are between about 700 and 800 K. In addition, both figures 3 and 4 show that the faster the quenching rate, the higher the glass transition temperature, which is consistent with experimental findings [4, 21]. This is because faster cooling results in less time for the atoms to relax, thus leading to the formation of the glass at a higher temperature than that with a lower cooling rate.

For the cooling rate of 2.0 K ps^{-1} in figure 3, it can be seen that the energy curve is different from both those energy curves showing crystallization and those energy curves showing glass formation. It seems that under this cooling rate the final phase is a glass structure with a little crystallization. This is further confirmed by the RDF at room temperature in figure 5. The RDF with the cooling rate of 1.0 K ps^{-1} shows a typical crystal structure, while the RDF with the cooling rate of 10 K ps^{-1} shows a typical amorphous structure. For the RDF with the cooling rate of 2.0 K ps^{-1}, it can be seen that although the second peak in the RDF has split into two subpeaks indicating glass transition, the left subpeak is significantly higher than the right subpeak, which shows that the final phase is a partially crystallized amorphous structure.

In order to examine the structural change during heating, the final solidified structures obtained with the different cooling rates were heated up again with a heating rate of 1 K ps^{-1}. Figure 6 shows the internal energy change during heating for three typical cases of A, B and

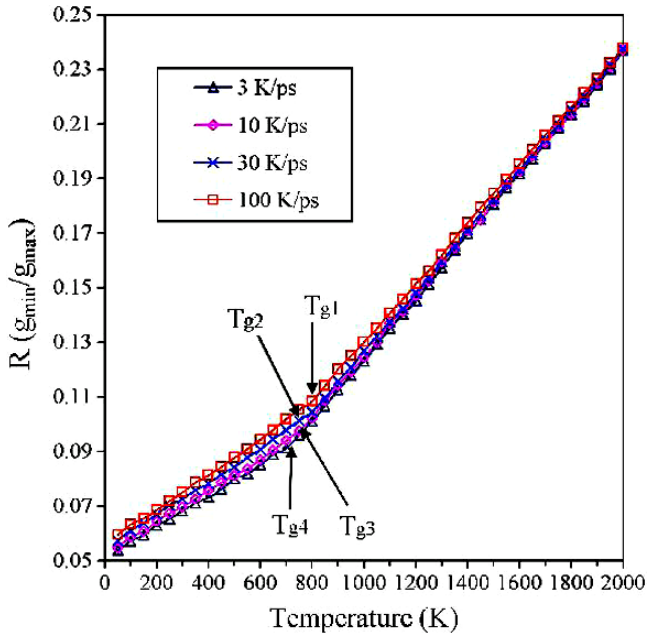

Figure 4. Variation of the Wendt–Abraham parameter R during cooling. The glass transition temperatures (T_g) are shown by arrows.

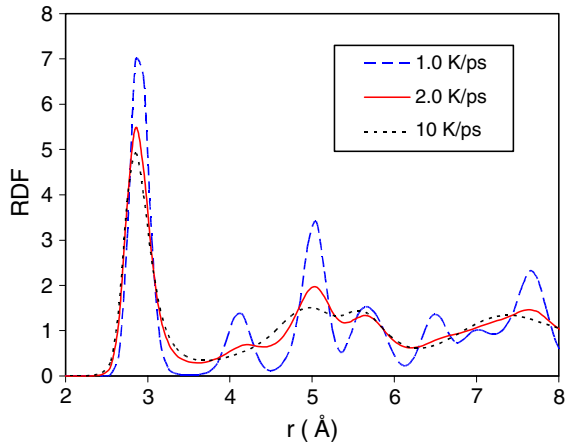

Figure 5. The radial distribution functions at room temperature after cooling down at the rates of 1.0, 2.0, and 10 K ps^{-1}, respectively.

C, which are heated with the solidified structure at the cooling rates of 1.0, 2.0 and 10 K ps^{-1}, respectively. It can be seen that the three different solidified structures result in different internal energy changes during the heating processes. For case A, as the starting structure is crystalline, the internal energy increases linearly with the temperature rise until there is an energy jump, which indicates the melting of the solid. The melting temperature T_m is defined in figure 6, which is about 1800 K. For case C, as the starting structure is amorphous, there is an energy drop at about 810 K, which shows that crystallization occurred before melting.

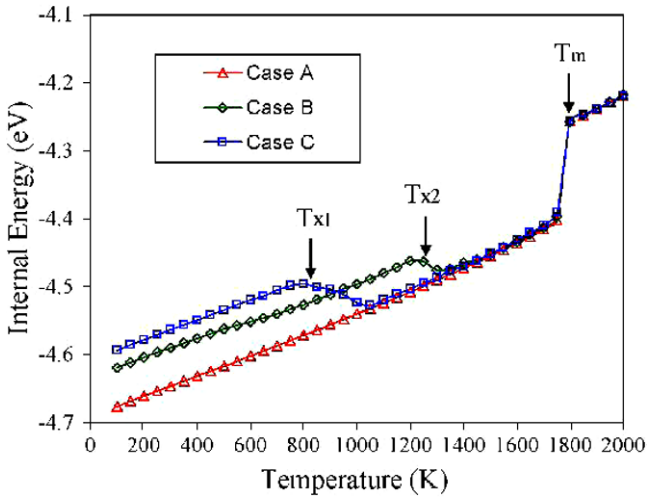

Figure 6. Variation of internal energy during the heating process. Cases A, B, and C are heated with the solidified structures obtained at the cooling rates of 1.0, 2.0, and 10 K ps^{-1}, respectively. The crystallization temperatures (T_x) and melting temperature (T_m) are indicated by arrows.

For case B, it can be seen that the energy curve is similar to the energy curve of case C. As the starting structure of case B is an amorphous structure with partial crystallization, there is also an energy drop in case B during heating, which indicates a further crystallization. However, the crystallization temperature T_{x2} in case B is higher than T_{x1} in case C, which may be due to the fact that the partially crystallized amorphous structure in case B has lower internal energy than the fully amorphous structure in case C. The simulated crystallization temperatures for the totally amorphous structures (obtained with cooling rates 10 K ps^{-1} and above) are around 810 K, which is close to the experimental crystallization temperatures of 823 K in crystallizing amorphous Ti–Al alloy [22]. For all the cases, the simulated melting temperature T_m is about 5% lower than the experimental melting temperature of Ti_3Al, which may be due to the fact that the crystallized structure is not a perfectly ordered $D0_{19}$ lattice.

4. Summary and conclusions

Based on the EAM potential for the Ti–Al system that was recently developed by Zope and Mishin [17], we carried out NPT-MD simulations to study the phase transformations in Ti_3Al alloy during rapid cooling and subsequent heating processes. The simulation results show that faster cooling results in a more disordered structure with higher internal energy, while slower cooling favours the formation of a more stable structure with lower internal energy. We found that an amorphous structure was formed at the quenching rates of 3.0 K ps^{-1} and above, while a crystalline structure was formed at the quenching rates of 1.5 K ps^{-1} and below. At the quenching rate of 2.0 K ps^{-1}, an amorphous structure with partial crystallization was obtained. For the high quenching rates of 3.0–100 K ps^{-1}, the corresponding glass transition temperature was obtained to be between 700 and 800 K. The simulation results also show that the faster the cooling, the higher the glass transition temperature, which is consistent with experimental results [4, 21].

When the final solidified structures obtained with the various cooling rates were heated up, different structural changes were observed. The amorphous structure undergoes crystallization

during heating and thus the crystallization temperature is identified, which is close to the experimental crystallization temperature. The simulated melting temperature is about 5% lower than the standard melting temperature, which may be due to the fact that the crystallized Ti_3Al does not have a perfect ordered $D0_{19}$ lattice structure.

Acknowledgment

This work was supported by the Agency for Science, Technology and Research (A*Star), Singapore.

References

[1] Jacobson L A and McKittrick J 1994 *Mater. Sci. Eng. Rep.* **11** 355
[2] Suryanarayana C 1999 *Non-Equilibrium Processing of Materials* (Amsterdam: Pergamon)
[3] Li G X, Liang Y F, Zhu Z G and Liu C S 2003 *J. Phys.: Condens. Matter* **15** 2259
[4] Liu C S, Zhu Z G, Xia J and Sun D Y 2001 *J. Phys.: Condens. Matter* **13** 1873
[5] Qi Y, Cagin T, Kimura Y and Goddard W A 1999 *Phys. Rev.* B **59** 3527
[6] Shimono M and Onodera H 2001 *Mater. Sci. Eng.* A **304–306** 515
[7] Cong H R, Bian X F, Zhang J X and Li H 2002 *Mater. Sci. Eng.* A **326** 343
[8] Wang L, Bian X and Yang H 2002 *Phys. Lett.* A **302** 318
[9] Noya E G, Rey C and Gallego L J 2002 *J. Non-Cryst. Solids* **298** 60
[10] Asta M, Morgan D, Hoyt J J, Sadigh B, Althoff J D, Fontaine D and Foiles S M 1999 *Phys. Rev.* B **59** 14271
[11] Daw M S, Foiles S M and Baskes M I 1993 *Mater. Sci. Rep.* **9** 251
[12] Finnis M W and Sinclair J E 1984 *Phil. Mag.* A **50** 45
[13] Daw M S and Baskes M J 1983 *Phys. Rev. Lett.* **50** 1285
[14] Daw M S and Baskes M J 1984 *Phys. Rev.* B **29** 6443
[15] Baskes M I, Asta M and Srinivasan S G 2001 *Phil. Mag.* A **81** 991
[16] Belonoshko A B, Ahuja R, Eriksson O and Johansson B 2000 *Phys. Rev.* B **61** 3838
[17] Zope R R and Mishin Y 2003 *Phys. Rev.* B **68** 024102
[18] Waseda Y 1980 *The Structure of Non-Crystalline Materials, Liquid and Amorphous* (New York: McGraw-Hill)
[19] Villars P 1997 *Person's Handbook of Crystallographic Data for Intermetallic Phase* (Metals Park, OH: ASM International)
[20] Wendt H R and Abraham F F 1978 *Phys. Lett.* **41** 1244
[21] Gaskell P H 1977 *The Structure of Non-Crystalline Materials* (London: Taylor and Francis)
[22] Banerjee R, Swaminathan S, Wiezorek J M K, Wheeler R and Fraser H L 1996 *Metall. Mater. Trans.* A **27** 2047